Matters Arising

Neuron

Lineage Tracing Using *Cux2-Cre* and *Cux2-CreERT2* Mice

Highlights

- Transgene expression patterns from the *Cux2* genetic locus depend on genetic background
- Cux2 is expressed in a subset of radial glial cells
- The vast majority of excitatory neocortical neurons fate mapped by Cux2-Cre are Satb2$^+$
- Cux2-CreERT2$^+$ progenitors in the E11.5 dorsal ventricular zone generate Satb2$^+$ neurons

Authors

Cristina Gil-Sanz, Ana Espinosa, ..., Santos J. Franco, Ulrich Müller

Correspondence

santos.franco@ucdenver.edu (S.J.F.), umueller@scripps.edu (U.M.)

In Brief

Gil-Sanz et al. show how genetic background can affect transgene expression in genetically modified mice, thus potentially affecting the interpretation of genetic fate-mapping results that are carried out with such transgenic lines.

Gil-Sanz et al., 2015, Neuron *86*, 1091–1099
May 20, 2015
http://dx.doi.org/10.1016/j.neuron.2015.04.019

CellPress

Neuron
Matters Arising

Lineage Tracing Using *Cux2-Cre* and *Cux2-CreERT2* Mice

Cristina Gil-Sanz,[1] Ana Espinosa,[1] Santiago P. Fregoso,[2] Krista K. Bluske,[1] Christopher L. Cunningham,[1] Isabel Martinez-Garay,[3] Hongkui Zeng,[4] Santos J. Franco,[2,5,6,*] and Ulrich Müller[1,*]
[1]Molecular and Cellular Neuroscience Department, Dorris Neuroscience Center, The Scripps Research Institute, La Jolla, CA 92037, USA
[2]Graduate Program in Cell Biology, Stem Cells and Development, University of Colorado School of Medicine, Aurora, CO 80045, USA
[3]Department of Physiology, Anatomy, and Genetics, University of Oxford, Oxford OX1 3QX, UK
[4]Allen Institute for Brain Science, Seattle, WA 98103, USA
[5]Department of Pediatrics, University of Colorado School of Medicine, Aurora, CO 80045, USA
[6]Program of Pediatric Stem Cell Biology, Children's Hospital Colorado, Aurora, CO 80045, USA
*Correspondence: santos.franco@ucdenver.edu (S.J.F.), umueller@scripps.edu (U.M.)
http://dx.doi.org/10.1016/j.neuron.2015.04.019

SUMMARY

Using genetic fate-mapping with *Cux2-Cre and Cux2-CreERT2* mice we demonstrated that the neocortical ventricular zone (VZ) contains radial glial cells (RGCs) with restricted fate potentials (Franco et al., 2012). Using the same mouse lines, Guo et al. (2013) concluded that the neocortical VZ does not contain lineage-restricted RGCs. We now show that the recombination pattern in *Cux2-Cre/CreERT2* mice depends on genetic background and breeding strategies. We provide evidence that Guo et al. likely reached different conclusions because they worked with transgenic sublines with drifted transgene expression patterns. In *Cux2-Cre* and *Cux2-CreERT2* mice that recapitulate the endogenous *Cux2* expression pattern, the vast majority of fate-mapped neurons express Satb2 but not Ctip2, confirming that a restricted subset of all neocortical projection neurons belongs to the *Cux2* lineage. This Matters Arising paper is in response to Guo et al. (2013), published in *Neuron*. See also the Matters Arising Response paper by Eckler et al. (2015), published concurrently with this Matters Arising in *Neuron*.

INTRODUCTION

We identified an RGC lineage in the neocortex that expresses the *Cux2* gene and is fate restricted (Franco et al., 2012). Using *Cux2-Cre* mice for cumulative lineage-tracing studies, we reported that 75% of all neurons in the *Cux2-Cre* lineage are found in upper neocortical cell layers and 25% in lower layers (Franco et al., 2012). Most neurons of the *Cux2-Cre* lineage expressed Satb2 (Franco et al., 2012), which is used as a marker for callosal projection neurons in upper and lower layers and for locally projecting neurons in layer 4 (Alcamo et al., 2008; Arlotta et al., 2005; Britanova et al., 2008). We will refer to these neurons as corticocortical projection neurons. Some cells in the *Cux2-Cre* lineage expressed the interneuron marker Gad65/67 and few cells were positive for Ctip2 (Franco et al., 2012), which is expressed in interneurons and in corticofugal projection neurons (Arlotta et al., 2005; Franco et al., 2012). Similar observations were made when we used *Cux2-CreERT2* mice and tamoxifen injections at E10.5 for temporal genetic fate-mapping (Franco et al., 2012), indicating that progenitors expressing *Cux2-CreERT2* at E10.5 are fate restricted.

Using similar strategies, Guo et al. (2013) found no evidence for fate-restricted RGCs. Here we have addressed this discrepancy and provide a likely explanation why Guo et al. reached a conclusion different from ours. We show that the recombination pattern in *Cux2-Cre/CreERT2* mice depends on genetic background and breeding strategies. Specifically, repeated sibling interbreedings of mice carrying the transgene on the C57BL/6 genetic background lead to progressive changes in the expression pattern of transgenes from the *Cux2* locus that no longer reflects endogenous *Cux2* expression. Changes in the expression pattern of the transgene are also observed on different genetic backgrounds. Notably, *Cux2-Cre/CreERT2* mice obtained by the Chen laboratory originally came from colonies that were maintained for over 10 generations (> 3 years) by interbreeding mice homozygous for the transgene, which we show here affects the Cre expression pattern. Analysis of the results presented in Eckler et al. (2015) in this issue of *Neuron* suggests that the Chen laboratory is working with a *Cux2-CreERT2* subline with a recombination pattern that no longer recapitulates the expression pattern of the endogenous *Cux2* locus. Importantly, by breeding mice with the aberrant transgene expression pattern onto different genetic backgrounds, the recombination pattern that recapitulates the expression pattern of the endogenous *Cux2* genetic locus can be reestablished. Using these "recovered" mice as well as additional fate-mapping strategies, we provide further evidence supporting the conclusion that the neocortical VZ contains fate-restricted progenitors.

RESULTS

The *Cux2* Genetic Locus Exhibits Variable Activity that Depends on Genetic Background and Is Active in the Developing Germline

All animal procedures were performed using Institutional Animal Care and Use Committees (IACUC)-approved protocols that

adhere to the standards of the NIH. *Cux2-Cre* and *Cux2-CreERT2* mice were generated on a *C57BL/6* background (Franco et al., 2012, 2011). For experimentation we routinely used heterozygous $Cux2^{+/Cre}$ and $Cux2^{+/CreERT2}$ mice maintained by breeding to wild-type *C57Bl/6* mice. When crossed to different Cre reporter lines on a congenic *C57Bl/6J* background, $Cux2^{+/Cre}$ mice consistently exhibited a recombination pattern that recapitulated the upper-layer-biased expression pattern of the endogenous *Cux2* gene (Figure 1A).

To facilitate maintenance of the lines for frequent shipments, we generated homozygous $Cux2^{Cre/Cre}$ or $Cux^{CreERT2/CreERT2}$ mice. Mice that were ultimately obtained by the Chen laboratory were maintained for more than ten generations of interbreeding in our homozygous colony. Significantly, when we crossed these inbred $Cux2^{Cre/Cre}$ mice to the $Ai9^{fl/fl}$ reporter, their offspring often exhibited sparse recombination patterns (Figure 1B; "Sparse") that spanned all neocortical cell layers equally (Figures 1B and 1E). This was in stark contrast to the expression pattern of the endogenous *Cux2* genetic locus and the recombination pattern in *Cux2-Cre* mice that were not maintained by breeding homozygous littermates (Figure 1A) (Franco et al., 2012). We observed this shifted recombination pattern with increasing magnitude and frequency upon prolonged inbreeding of $Cux2^{Cre/Cre}$ mice. The aberrant recombination pattern was stably inherited even when the mice were subsequently crossed to *C57BL/6J* wild-type mice to generate $Cux2^{+/Cre}$ heterozygotes. This suggests that once established, the epigenetic changes at the genetically modified *Cux2* locus are stably inherited in the *C57BL/6J* genetic background. To test whether the expression pattern could be reset on a different genetic background, we outcrossed inbred $Cux2^{Cre/Cre}$ mice with the outbred strain *ICR* for three generations. We then crossed the resulting $Cux2^{+/Cre}$ mice to $Ai9^{fl/fl}$ mice and found that we recovered the original upper-layer-biased pattern (Figure 1B; "Recovered").

We also observed that crossing inbred $Cux2^{Cre/Cre}$ mice to the *Rosa26-NZG* reporter line on an *FVB/NJ* background resulted in a recombination pattern that was much broader than the original pattern (Figure 1C). This expanded pattern was seen in all brain regions, including the neocortex and hippocampus (Figure 1C), and included all neocortical cell layers (Figure 1F). The original pattern was recovered when $Cux2^{Cre/Cre}$ mice were outbred onto the *FVB/NJ* background for five generations (Figures 1D and 1F). These data indicate that the recombination pattern in *Cux2-Cre* mice is subject to differences in genetic background of the parents carrying the Cre and/or Cre-reporter transgenes.

We also collaborated with The Jackson Laboratory and the Allen Institute for Brain Science to characterize *Cux2-Cre* and *Cux2-CreERT2* mice for the Allen Brain Atlas (ABA) website (www.brain-map.org). Mice that were shipped to The Jackson Laboratory and Allen Institute had been maintained by homozygous inbreeding for three to four generations. *Cux2-Cre* mice maintained by homozygous breedings for a few generations exhibited layer-specific recombination throughout different functional domains of the neocortex (Figures S1A and S1C), although some brains showed a somewhat broadened expression pattern especially in the lateral cortex (not shown). This broadened expression was likely caused by genetic drift caused by inbreeding of the *Cux2-Cre* homozygous mice for a few generations. Surprisingly, some brains on the ABA website displayed uniform recombination throughout the whole brain, including all neocortical cell layers (Figure S1D, not shown). Mice with this broad recombination pattern inherited *Cux2-Cre* and the Cre-reporter allele from the same parent (Figure S1B; "Breeding Strategy 2"). We hypothesized that *Cux2-Cre* is expressed in the developing F1 germline where it drives recombination of the reporter, thus leading to inheritance of the recombined reporter allele in F2 progeny (Figure S1B). Indeed, breeding *Cux2-Cre;Ai9* double heterozygous mice to WT mice led to ubiquitous reporter gene expression throughout the entire animal in F2 progeny (Figures S1E and S1F). This was true even in F2 animals that did not inherit *Cux2-Cre* (Figures S1E and S1F), indicating F1 germline recombination. Not all F2 embryos exhibited ubiquitous recombination (Figures S1D and S1E), indicating mosaic germline recombination. We confirmed that breeding *Cux2-Cre;Rosa-NZG* double heterozygous F1 mice to WT animals produced similar results, with some F2 embryos exhibiting ubiquitous recombination even in the absence of the Cre allele (Figure S1G). Future releases of the ABA website will include information to specify the breeding scheme and inheritance pattern of the *Cux2-Cre* and Cre-reporter alleles.

We conclude that the expression pattern of the *Cre* transgene in *Cux2-Cre/CreERT2* mice is dependent on genetic background and breeding scheme.

Cux2-Cre Mice Mark a Subset of Neocortical Projection Neurons

To confirm our original lineage-mapping results (Franco et al., 2012), we performed additional analyses using *Cux2-Cre* mice that were continuously maintained by breedings of heterozygous *Cux2-Cre* mice with C57BL/6 wild-type mice, a breeding scheme that maintains the same expression pattern for Cre as for the endogenous Cux2 gene as determined by in situ hybridization (Franco et al., 2012; Nieto et al., 2004; Zimmer et al., 2004). We analyzed recombination in the mediolateral part of the neocortex along its rostrocaudal extent at embryonic days (E) 10.5, E12.5, and E14.5. As reported (Franco et al., 2012), *Cux2-Cre* induced recombination in a subset of Pax6-positive RGCs that increased in numbers from E10.5 to E14.5 (Figures S2A and S2B). Cre protein was present in the recombined progenitors (Figure S2C). We then analyzed brains at postnatal day (P) 30 along the rostrocaudal extent of the brain. A *Nex/Neurod6-Cre* control transgene that induces recombination in nearly all neocortical projection neurons (Belvindrah et al., 2007a; Wu et al., 2005) labeled neurons equally in all cell layers (Figure S2D). *Cux2-Cre* mice exhibited recombination extensively in upper neocortical cell layers and much less in lower layers (Figure S2D). Some signal in lower layers is expected because *Cux2-Cre*-mediated recombination labels interneurons that reside in all cell layers and $Satb2^{+}$ projection neurons that reside in upper and, to a lesser extent, lower layers (Franco et al., 2012). In addition, the *Ai9* reporter exhibited a diffuse signal in lower layers consistent with the fact that tdTomato is expressed in the processes of upper-layer projection neurons that arborize in lower layers. However, fluorescence in

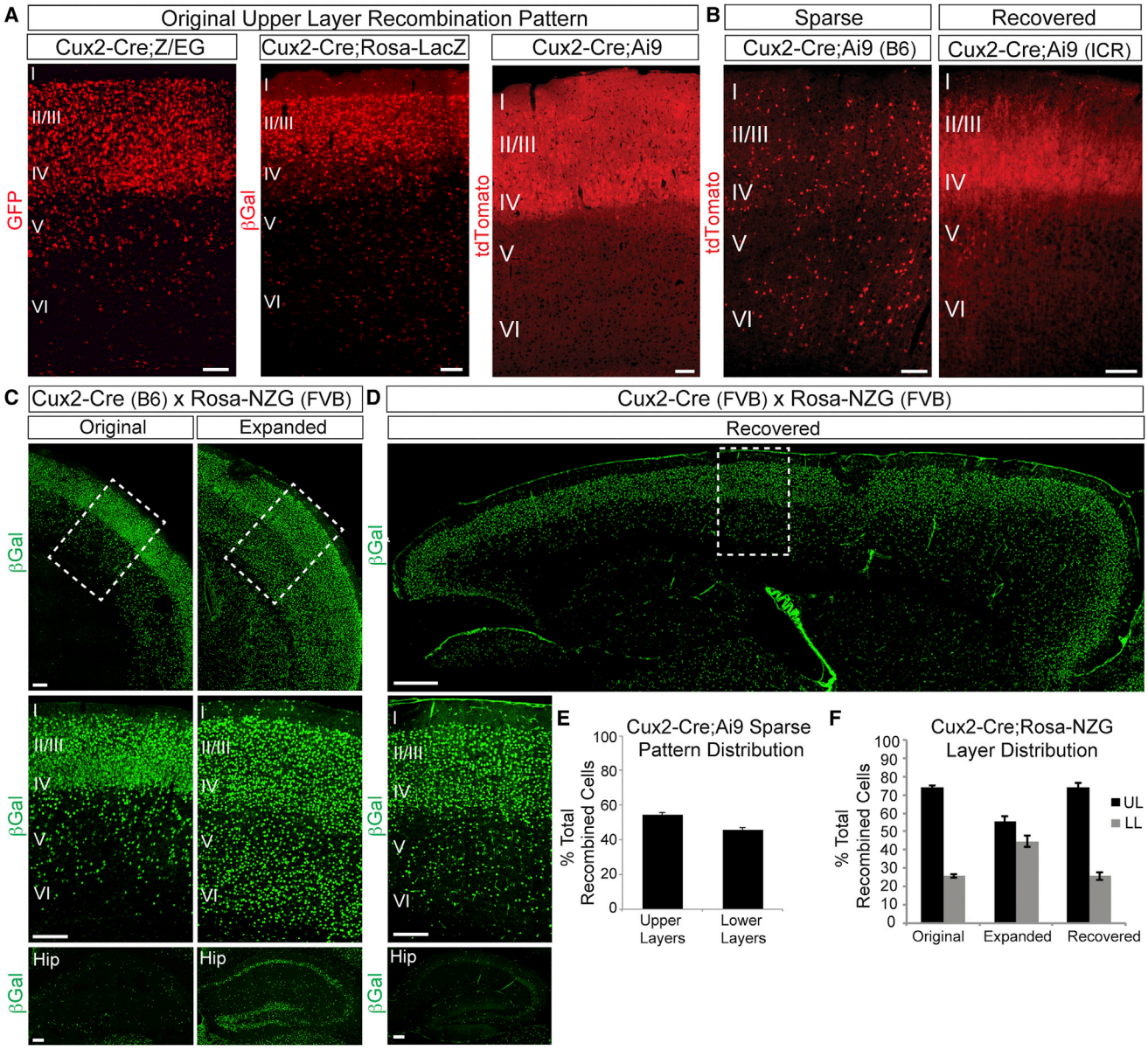

Figure 1. The *Cux2* Genetic Locus Exhibits Variable Activity that Depends on Genetic Background

(A) Coronal sections from *Cux2-Cre* mice crossed to Cre reporter lines (all on a congenic *C57BL/6J* background). Note recombination primarily in upper neocortical layers, with some scattered cells in lower layers.

(B) Coronal sections from *Cux2-Cre* mice crossed to the *Ai9* reporter showing sparse recombination in the homozygous inbred line (left panel) and the recovered original pattern after outbreeding onto the *ICR* strain (right panel).

(C) Coronal sections from *Cux2-Cre;Rosa26-NZG* mice showing the original (left) and expanded (right) recombination patterns in the neocortex (top, middle) and hippocampus (bottom). Middle panels: enlarged images of boxed areas in top panels.

(D) Sagittal section from a *Cux2-Cre;Rosa26-NZG* mouse showing the recovered original recombination pattern in the neocortex (top, middle) and hippocampus (bottom) after outbreeding *Cux2-Cre* onto an *FVB/NJ* background for five generations. Middle panel is enlarged image of boxed area in top panel.

(E) Quantification (mean ± SEM) of layer distribution of tdTomato$^+$ cells in sparsely recombined *Cux2-Cre;Ai9* mice (502 cells from three animals).

(F) Quantification (mean ± SEM) of the layer distribution of βGal$^+$ cells in *Cux2-Cre;Rosa26-NZG* mice exhibiting the different recombination patterns in (C) and (D).

Scale bars: (A) and (B), 100 μm; (C), 200 μm; (D), 500 μm (top) and 200 μm (middle, bottom).

cell bodies was distinguished from that in the neuropil by confocal microscopy, which revealed no fluorescence in the majority of pyramidal neurons in lower layers (Figure S2E). These data are consistent with our earlier publication (Franco et al., 2012) and confirm that when genetic background is carefully controlled, *Cux2-Cre* mice are a useful tool to determine the full complement of cells that express *Cre* from the *Cux2* locus at any point during their development and maturation.

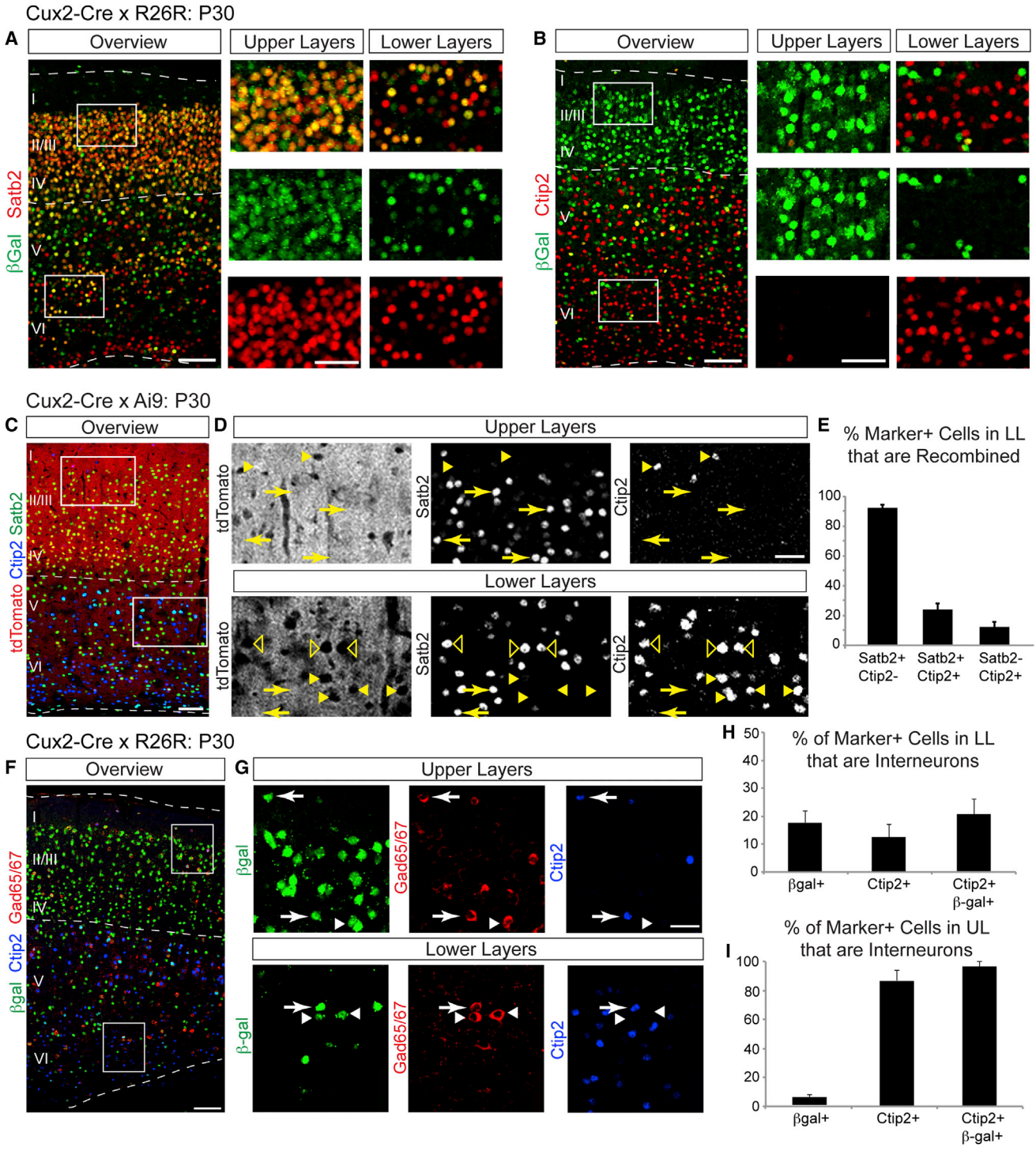

Figure 2. *Cux2-Cre* Cumulative Fate-Mapping Labels Satb2$^+$ Corticocortical Projection Neurons

(A and B) Sagittal sections from *Cux2-Cre;Rosa-LacZ* adult brains immunostained for βGal (green) to reveal recombined cells and for two projection neuron markers (red): Satb2, corticocortical; Ctip2, corticospinal. Note the high degree of co-localization between βGal and Satb2 (A) and modest co-localization of βGal with Ctip2 (B).

(C) Coronal section from a *Cux2-Cre;Ai9* adult neocortex immunostained for Satb2 (green) and Ctip2 (blue). tdTomato fluorescence (red) marks recombined cells.

(D) Higher-magnification views of boxed regions in (C). Labeled are examples of Satb2$^+$ (arrows), Ctip2$^+$ (arrowheads), and Satb2$^+$/Ctip2$^+$ cells (empty arrowheads).

(legend continued on next page)

To define the subtype of neurons fate-mapped with the *Cux2-Cre* line, we analyzed *Cux2-Cre;Rosa26R-LacZ* for co-expression of βGal with Satb2, a marker for corticocortical projection neurons (Alcamo et al., 2008; Britanova et al., 2008) and with Ctip2 and Tle4, markers for subsets of corticofugal projection neurons (Arlotta et al., 2005; Koop et al., 1996). β-gal protein in the *Rosa26R-LacZ* reporter is strongly expressed in cell bodies, thus facilitating the identification of individual cells. Consistent with our previous study (Franco et al., 2012), the vast majority of cells fate mapped by *Cux2-Cre* expressed Satb2 (Figure 2A) but not Ctip2 (Figure 2B) or Tle4 (not shown). We next extended our analyses to the *Ai9* tdTomato reporter (Madisen et al., 2010) for better comparison with Guo et al. (2013). We used Satb2 and Ctip2 as markers of corticocortical and corticofugal projection neurons, respectively (Figures 2C and 2D). There was strong overlap between Satb2 and tdTomato in upper and lower layers (Figure 2D). Since essentially all projection neurons in upper layers are Satb2$^+$ and Ctip2$^-$ (Alcamo et al., 2008; Britanova et al., 2008), we performed quantitative analysis on recombined cells in lower layers in serial sections. We analyzed 2,902 cells in three animals, focusing on the medio-lateral part of the neocortex that primarily comprises the somatosensory cortex. We counted total numbers of Satb2$^+$/Ctip2$^-$, Satb2$^+$/Ctip2$^+$, and Satb2$^-$/Ctip2$^+$ cells and determined within each category the percentage that were recombined (Figure 2E). Of all lower-layer Satb2$^+$/Ctip2$^-$ cells, 92% ± 4% belonged to the *Cux2-Cre* lineage. Only 12% ± 6% of all Ctip2$^+$/Satb2$^-$ cells in lower layers were recombined. Of the Satb2$^+$/Ctip2$^+$ population, 24% ± 7% belonged to the *Cux2-Cre* lineage; we speculate that this is a poorly characterized projection neuron population that cannot be defined as corticocortical or corticofugal by staining for Satb2 and Ctip2.

During development, *Cux2* is expressed in some migrating interneurons (Zimmer et al., 2004). Consistent with this and with our earlier findings (Franco et al., 2012), we found that 10% of all cells in the *Cux2-Cre* lineage expressed the interneuron marker Gad65/67 (Figures 2F–2I and S2F; 6% in upper layers and 17% in lower layers). Since Ctip2 is expressed in a subset of interneurons (Figures 2F–2I; 86% of Ctip2$^+$ cells in upper layers and 12% in lower layers are Gad65/67$^+$), some recombined Ctip2$^+$ cells might be interneurons. We quantified the number of Ctip2$^+$ interneurons within the *Cux2-Cre* lineage (1,240 cells analyzed in two animals). Twenty-one percent of recombined Ctip2$^+$ cells in lower layers were interneurons (Figure 2H). In upper layers, nearly all recombined Ctip2$^+$ cells were interneurons (Figure 2I).

Our *Cux2-Cre* data were in stark contrast to the patterns in *Neurod6-Cre* and *Emx1-Cre*, which drive recombination in all neocortical projection neurons but not interneurons (Belvindrah et al., 2007b; Gorski et al., 2002; Wu et al., 2005). Ninety percent and eighty-eight percent of all Ctip2$^+$ cells belonged to the *Neurod6-Cre* and *Emx1-Cre* lineages, respectively, whereas only 7% of all Ctip2$^+$ cells belonged to the *Cux2-Cre* lineage (many of which are interneurons) (Figure S2G). Thus, unlike in fate-mappings with *Neurod6-Cre* and *Emx1-Cre*, very few cells in the *Cux2* lineage are Ctip2$^+$/Satb2$^-$ corticofugal projection neurons.

We reported that astrocytes were not detected in the *Cux2-CreERT2* fate-mapped lineage at P10 (Franco et al., 2012). If *Cux2*$^+$ progenitors generate astrocytes at the end of upper-layer neurogenesis, P10 may be too early a time point to observe late-born, morphologically mature astrocytes. We therefore analyzed later time points in *Cux2-Cre;Ai9* animals using an antibody against the astrocyte marker Aldh1L1. Only a minor fraction of Aldh1L1$^+$ astrocytes were within the *Cux2-Cre* fate-mapped lineage (Figure S2H).

These data confirm our published findings (Franco et al., 2012), which concluded that the vast majority of excitatory neurons in the *Cux2-Cre* lineage are Satb2$^+$ projection neurons that are abundant in upper neocortical cell layers but can also be found in lower layers. In agreement with published findings (Franco et al., 2012; Zimmer et al., 2004), *Cux2-Cre* also labels a subset of interneurons and a minor fraction of Ctip2$^+$ projection neurons and neocortical astrocytes. In light of our discovery that expression of transgenes from the *Cux2* locus is dependent on genetic background and breeding strategies, the discrepancy between our study (Franco et al., 2012) and that of the Chen laboratory (Guo et al., 2013) is likely explained by altered recombination patterns caused by differences in genetic background and breeding strategies used to maintain the *Cux2-Cre* and *Cux2-CreERT2* lines.

Temporal Genetic Fate-Mapping Using *Cux2-CreERT2* Mice Identifies a Population of Fate-Restricted RGCs

Like other mice that constitutively express Cre, *Cux2-Cre* mice do not inform about the time point when recombination occurs. Inducible genetic fate-mapping using CreERT2 allows for temporal control over recombination by activating recombination with tamoxifen at defined time points to investigate progenitor-offspring relationships (Hayashi and McMahon, 2002; Zervas et al., 2004). We showed previously that an early E10.5 injection of tamoxifen into *Cux2-CreERT2;Ai9* mice labeled RGCs that gave rise to neurons in the P10 neocortex that predominantly resided in upper neocortical layers (Franco et al., 2012). To extend these findings, we injected the faster-acting and shorter-lived tamoxifen metabolite 4-hydroxy-tamoxifen (4-OHT) (Guenthner et al., 2013) into *Cux2-CreERT2;Ai9* animals at E10.5 and E11.5: time-points when intermediate progenitors (IPs) and differentiated neurons, including interneurons, are

(E) Percentage of recombined lower-layer cells that express Satb2 and/or Ctip2 in the adult neocortex (mean ± SEM); 2,902 cells from three animals were quantified.

(F) Sagittal section from a *Cux2-Cre;Rosa-LacZ* adult neocortex immunostained for βGal to reveal recombined cells (green), Gad65/67$^+$ interneurons (red), and Ctip2 (blue).

(G) Higher-magnification views of the boxed regions in (F). Some recombined cells are Gad65/67$^+$ (arrows and arrowheads) and a subset of these are Ctip2$^+$ (arrows).

(H and I) Percentage of interneurons expressing indicated markers (mean ± SEM); 1,240 cells from two animals were quantified. Scale bars: (A)–(C) and (F), 100 μm; 50 μm in boxed insets; (D) and (G), 50 μm.

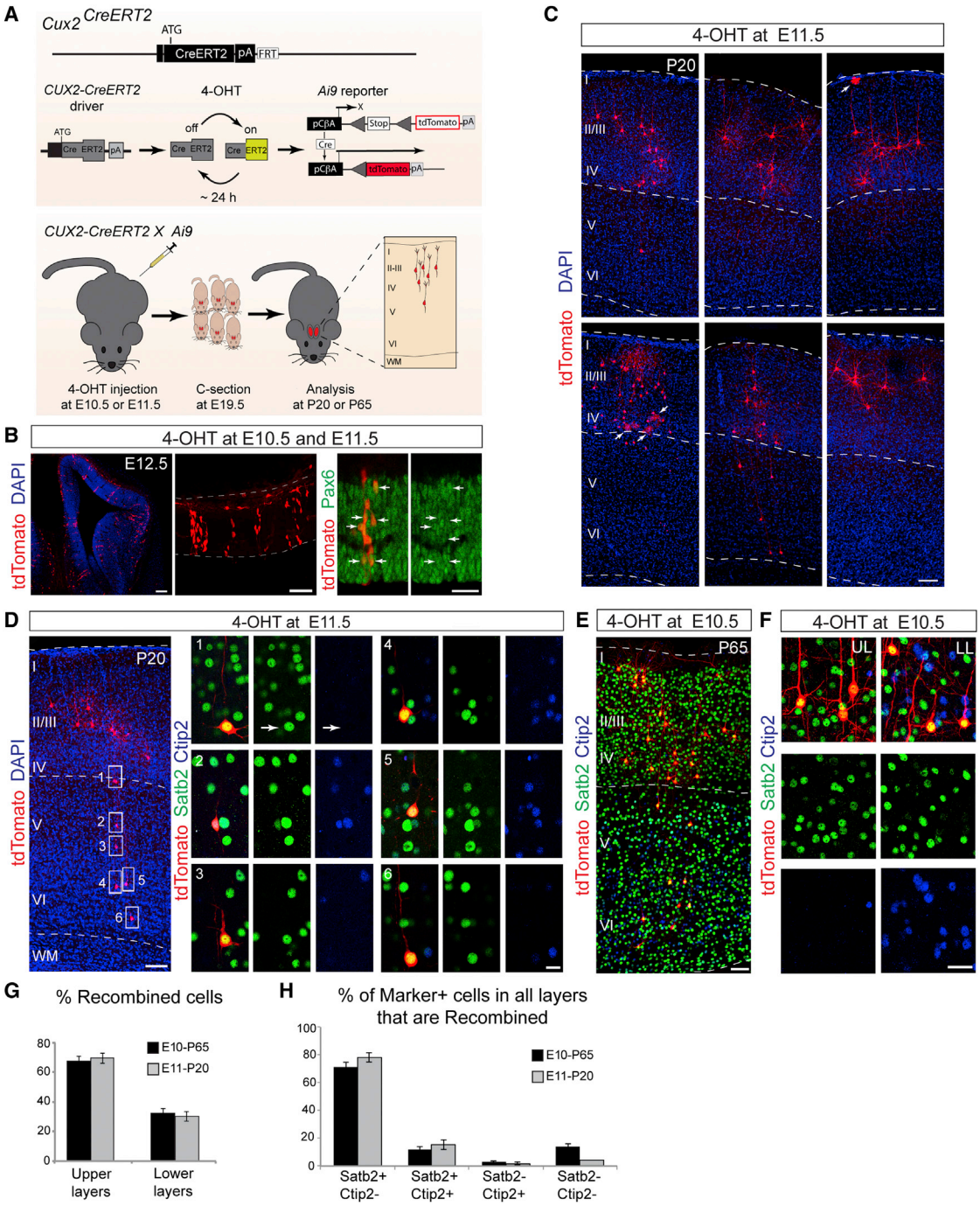

Figure 3. Temporal Genetic Fate-Mapping Using *Cux2-CreERT2* Mice

(A) Targeting strategy for *Cux2-CreERT2* mice and fate-mapping strategy. Pregnant dams were injected with 4-OHT at the indicated times. Pups were delivered by C-section at E19.5 and transferred to foster mothers. Brains were analyzed at the indicated times.

(B) Confocal images showing the recombination pattern in the *Cux2-CreERT2;Ai9* neocortex at E12.5 after 4-OHT injections at E10.5 and E11.5. Recombined cells in the VZ express Pax6 (arrows).

(C) Neocortex from *Cux2-CreERT2;Ai9* animals injected with 4-OHT at E11.5 and analyzed at P20. Most recombined tdTomato$^+$ cells (red) are located in upper layers. Astrocytes were occasionally observed (arrows). Nuclei are stained with DAPI (blue).

(D) Example of a 4-OHT injection in which an isolated "clone" (red) contains neurons that reside in upper and lower layers. Note that all boxed cells in lower layers V-VI are Satb2$^+$ (green), whereas none express exclusively Ctip2 (blue).

(E) Neocortex from *Cux2-CreERT2;Ai9* animals injected with 4-OHT at E10.5 and analyzed at P65 for Satb2 (green) and Ctip2 (blue) expression in recombined tdTomato$^+$ cells (red).

(legend continued on next page)

largely absent from the emerging neocortex (Figure 3A). As shown for tamoxifen induction (Franco et al., 2012), a subpopulation of Pax6$^+$ RGCs in the VZ expressed tdTomato one day after injection of 4-OHT (Figure 3B), confirming recombination in progenitors. CreERT2 was active in the 4-OHT-injected animals for only a short time period. Two days after 4-OHT injection into *Cux2-CreERT2* pregnant dams, we used in utero electroporation to introduce a Cre-responsive EGFP-expression plasmid into the VZ of the embryos. When we analyzed the brains two days later, we did not observe reporter activation (Figures S3A–S3C). In controls, the same Cre-responsive EGFP-expression plasmid was activated in the presence of constitutively active Cre (data not shown; Franco et al., 2012). Thus, in experiments with *Cux2-CreERT2* mice recombination was induced in progenitors within one day of 4-OHT administration but not in differentiated neurons that emerge several days later.

We next analyzed the distribution and molecular identities of fate-mapped cells in mature brains at P20 and P65. A large fraction of cells derived from the *Cux2-CreERT2*$^+$ progenitor lineage were located in upper layers, with a smaller number of recombined cells settling in lower layers (Figures 3C–3F). The distribution of cells in upper and lower layers (Figure 3G) was similar to the distribution of cells cumulatively fate-mapped with *Cux2-Cre* (Franco et al., 2012). The identities of the cells in the *Cux2-CreERT2* lineage were determined using molecular markers to quantify 1,745 cells in serial sections from nine animals (Figures 3D–3F and 3H). Even among cells positioned in lower layers, nearly all recombined cells were Satb2$^+$ (Figure 3H; > 80% for E10.5 injections analyzed at P65; > 90% for E11.5 injections analyzed at P20). Some recombined cells expressed Ctip2, but most of these co-expressed Satb2 (Figure 3H). Only 2%–3% of recombined cells were Ctip2$^+$ and Satb2$^-$. In agreement with cumulative fate-mapping results, some of the recombined cells in lower layers were interneurons (Figures S3D–S3H).

Consistent with earlier findings (Franco et al., 2012), we rarely found astrocytes in the *Cux2-CreERT2* lineage in P10 brains following 4-OHT injections at E10.5 (Figure S2I). Recombined astrocytes were detected at P20 (Figure 3C, arrows) and more frequently at P65 (Figure S2I). This is consistent with the late postnatal local proliferation of astrocytes in the neocortex (Ge et al., 2012) and suggests that the small pool of astrocytes in the *Cux2-CreERT2* fate-mapped lineage is amplified postnatally by proliferation.

In summary, our temporal genetic fate-mapping results provide evidence that neocortical progenitors of the *Cux2-CreERT2* lineage that are labeled around E10.5–E11.5 generate predominantly Satb2$^+$ projection neurons, as well as interneurons and a minor population of astrocytes.

DISCUSSION

The study by Guo et al. (2013) has raised concerns regarding the fate-restriction of *Cux2-Cre*$^+$ progenitors. Although the interpretation of their data was confounded by the fact that they analyzed cell lineage in the immature cortex, a further likely explanation for this discrepancy is that the Chen laboratory used *Cux2-Cre/CreERT2* mice that no longer expressed Cre in a pattern reflecting that of the endogenous *Cux2* locus, as a result of breeding strategies and genetic background variations that likely can cause epigenetic changes at the genetically modified *Cux2* locus. The mice used by the Chen laboratory were derived from colonies in our laboratory that had been maintained by homozygous sibling matings for over ten generations (the mice were first shipped to Stanford from where they were imported to the Chen laboratory), a breeding scheme that we now show affects the expression pattern of the Cre transgenes. Once established, the shifted recombination patterns (Figures 1B and 1D) were maintained even in mice that were bred to *C57BL/6J* wild-type mice to obtain mice heterozygous for the transgenic locus, indicating that the epigenetic changes are stably inherited on the *C57BL/6J* background (but not following outbreeding to ICR mice). The shifted expression patterns exhibited equal distributions between upper and lower layers that closely resembled the distribution reported by Guo et al. (2013). Additionally, in their Matters Arising Response article (Eckler et al., 2015) the Chen laboratory achieved a very sparse "clone"-like recombination pattern in *Cux2-CreERT2* mice by injecting 4 mg tamoxifen per 40 g body weight, which is twice the amount that we used to induce robust widespread recombination throughout upper neocortical cell layers (Franco et al., 2012). Together these data suggest that the Chen laboratory is working with *Cux2-Cre/CreERT2* mice with shifted recombination patterns. Notably, at the time of shipment we were not aware of the effects of breeding scheme and genetic background on transgene expression from the *Cux2* locus.

By analyzing mice that exhibited reproducible recombination patterns recapitulating the expression pattern of the endogenous *Cux2* gene as determined by in situ hybridization, we provide further evidence that the VZ of the neocortex contains a subpopulation of RGCs that is fate restricted. Only a subset of RGCs express the *Cux2* gene and cumulative genetic fate-mapping experiments using *Cux2-Cre* mice demonstrate that the vast majority of the lineage-traced cells in the adult neocortex are Satb2$^+$ corticocortical projection neurons that are abundant in upper neocortical layers but can also be found in lower layers (Alcamo et al., 2008; Britanova et al., 2008). Using temporal genetic fate-mapping, we demonstrate that cells derived from *Cux2-CreERT2*$^+$ VZ progenitors generate predominantly Satb2$^+$ projection neurons, whereas the vast majority of Ctip2$^+$ neurons is derived from progenitors that do not belong to the *Cux2*$^+$ RGC lineage. Notably, although we used an unbiased approach to quantify cells in serial sections along the rostrocaudal axis from sparsely labeled brains, we cannot claim that we analyzed true clones derived from single progenitors. In this regard, we are concerned about the claim by Eckler et al. (2015) that they carried out a clonal analysis. Cell clones in their

(F) Higher-magnification view of the neocortex from *Cux2-CreERT2;Ai9* animals analyzed as in (E).
(G and H) Quantification of the layer distribution (G) and molecular marker expression (H) in isolated recombined "clones" in serial sections from injections at E10.5 and E11.5, analyzed at P65 and P20, respectively (mean ± SEM); 1,745 cells from nine animals were analyzed in "clones" that spanned several cell layers in serial sections. Scale bars: (B), left to right: 100, 100 and 50 μm; (C) and (E), 100 μm; (D), 100 μm; 25 μm for boxed insets; (F), 50 μm.

study spanned more than 0.5 mm along the rostrocaudal axis and the authors analyzed thousands of cells for each brain. This cell spread and density appears far too high to represent clones. This is a particularly important point for additional lineage-tracing studies carried out by Guo et al. (2013) and Eckler et al. (2015) using *FezF2-CreERT2* mice. The authors observed that in these mice cells in upper and lower layers were lineage traced. However, it is unclear from their analysis whether the cells in upper or lower layers were derived from single progenitors.

Guo et al. (2013) concluded that most cells in the *Cux2-Cre* lineage in the VZ are interneurons and that *Cux2-Cre* is not expressed in progenitors because they could not detect Cux2 protein in the VZ. However, we show that *Cux2-Cre* and *Cux2-CreERT2* induce recombination in a subset of $Pax6^+$ RGCs and that Cre protein is present in VZ progenitors. These data are consistent with in situ hybridization studies for *Cux2* that revealed expression of *Cux2* mRNA in RGCs and IPs in the VZ and SVZ (Franco et al., 2012; Nieto et al., 2004; Zimmer et al., 2004). Translation of the *Cux2* mRNA may be initiated later, as reported for other genes in the VZ/SVZ (Yang et al., 2014), or available antibodies may not be sensitive enough for detecting Cux2. Significantly, the number of proliferating IPs in the neocortex is increased in mice lacking *Cux2*, suggesting that Cux2 protein is expressed in progenitors and acts to restrain their proliferation (Cubelos et al., 2008). In this regard, we are surprised that interneurons appear absent in the lineage analysis carried out by Eckler et al. (2015), since they reported in their previous study (Guo et al., 2013) that interneurons are abundantly recombined with *Cux2-CreERT2* mice. Perhaps Cre was no longer expressed in interneurons in the mice used in the recent study (Eckler et al., 2015) due to changes in gene expression caused by breeding strategies.

We also show that the vast majority of neocortical neurons in the *Cux2-Cre* lineage of adult mice are $Satb2^+$ corticocortical projection neurons, some are interneurons, and only a very minor percentage are $Ctip2^+$ /$Satb2^-$ projection neurons. These data provide important insights into the total cell population that expresses Cre from the *Cux2* locus at any time during their development and provide evidence for restriction within the *Cux2-Cre* fate-mapped lineage. Notably, additional support for expression of Cux2 in a restricted subset of progenitors comes from functional studies. The *Dab1* gene regulates migration of projection neurons of all neocortical cell layers from the VZ into the cortical wall. When *Dab1* is inactivated with *Cux2-Cre*, migration of upper-layer neurons is disrupted, while deep-layer neurons are largely unaffected (Franco et al., 2011).

Our temporal genetic fate-mapping studies indicate that *Cux2-CreERT2*$^+$ progenitors in the neocortical VZ at E10.5–11.5 generate a restricted subset of neocortical projection neurons. Although we observed some variations in the number of fate-mapped projection neurons in upper layers ranging from 75% to 89%, which differed between functional cortical areas, the vast majority of neurons in the *Cux2-CreERT2* lineage in all cases expressed Satb2, a marker for corticocortical projection neurons (Fame et al., 2011; Molyneaux et al., 2009; Sohur et al., 2014). Variations in layer distribution may depend on functional domains of the neocortex and differences in experimental protocol (e.g., kinetics of tamoxifen versus 4-OHT) but do not change the conclusion that *Cux2-CreERT2*$^+$ progenitors are restricted in their fate potential.

A study using mosaic analysis with double markers (MADM) concluded that single RGCs in the *Emx1-CreERT2* lineage produced clones containing neurons with upper- and lower-layer identities (Gao et al., 2014). Notably, MADM depends on Cre-mediated interchromosomal mitotic recombination during the G2 phase of the cell cycle (Gao et al., 2014). Recombination efficiency will depend on cell-cycle length and on the genetic locus of the MADM reporter and thus likely does not capture all progenitor types with equal probability. Perhaps *Emx1-CreERT2* and MADM preferentially label a slowly proliferating multipotent progenitor subtype that subsequently generates various lineage-restricted progenitors with faster proliferation kinetics, including those labeled by *Cux2-CreERT2*. Surprisingly, Gao et al. (2014) concluded that during an asymmetric neurogenic division, a single RGC produces eight or nine neurons. This result is difficult to reconcile with studies using *Tbr2-Cre* to lineage-trace the output of IP cells (Vasistha et al., 2014). IPs are generated from RGCs and proliferate before generating neurons (Miyata et al., 2004; Noctor et al., 2004). Vasistha et al. (2014) concluded that IPs predominantly generate clones comprising > 16 cells. The observation that single *Emx1-CreERT2*$^+$ RGCs produce clones that are smaller than those traced by their IP offspring is difficult to explain but may reflect preferential labeling of a specific RGC sub-lineage with MADM.

In summary, we conclude that the neocortical VZ contains lineage-restricted progenitors around E10.5–11.5 that can be traced with *Cux2-CreERT2* mice. We further conclude that *Cux2-Cre* mice are a useful tool to trace the entire *Cux2*-lineage. It is critical when using these tools to control for genetic background, while also avoiding breeding schemes that allow for germline recombination.

EXPERIMENTAL PROCEDURES

All experimental procedures, genetic background of mice, and breeding schemes used in this article are presented in full in the Supplemental Information.

SUPPLEMENTAL INFORMATION

Supplemental Information includes Supplemental Experimental Procedures and three figures and can be found with this article online at http://dx.doi.org/10.1016/j.neuron.2015.04.019.

AUTHOR CONTRIBUTIONS

Conceptualization, C.G-S., S.J.F, and U.M.; Investigation, C.G-S., A.E., S.P.F., K.K.B., C.L.C., I.M-G., H.Z., and S.J.F.; Writing – Original Draft, C.G-S., S.J.F., and U.M.; Writing – Review & Editing, C.G-S., A.E., S.P.F., K.K.B., C.L.C., I.M-G., H.Z., S.J.F., and U.M.; Funding Acquisition, C.G-S., A.E., K.K.B., C.L.C., I.M-G., S.J.F., and U.M.

ACKNOWLEDGMENTS

This work was supported by the NIH (S.J.F., NS060355; U.M., NS046456, MH078833, HD070494), the Dorris Neuroscience Center (U.M.), the Skaggs Institute for Chemical Biology (U.M.), Children's Hospital Colorado Program in Pediatric Stem Cell Biology (S.J.F.), CIRM (A.E., C.-G.S., C.L.C., I.M.-G.),

a TSRI Stem Cell Postdoctoral Fellowship (K.K.B.), the Ministerio de Educacion (C.G.-S., EX2009-0416; I.M.-G., FU-2006-1238), and the Generalitat Valenciana (C.G.-S., APOSTD/2010/064).

Received: January 20, 2014
Revised: December 15, 2014
Accepted: March 30, 2015
Published: May 20, 2015

REFERENCES

Alcamo, E.A., Chirivella, L., Dautzenberg, M., Dobreva, G., Fariñas, I., Grosschedl, R., and McConnell, S.K. (2008). Satb2 regulates callosal projection neuron identity in the developing cerebral cortex. Neuron *57*, 364–377.

Arlotta, P., Molyneaux, B.J., Chen, J., Inoue, J., Kominami, R., and Macklis, J.D. (2005). Neuronal subtype-specific genes that control corticospinal motor neuron development in vivo. Neuron *45*, 207–221.

Belvindrah, R., Graus-Porta, D., Goebbels, S., Nave, K.-A., and Müller, U. (2007a). Beta1 integrins in radial glia but not in migrating neurons are essential for the formation of cell layers in the cerebral cortex. J. Neurosci. *27*, 13854–13865.

Belvindrah, R., Hankel, S., Walker, J., Patton, B.L., and Müller, U. (2007b). Beta1 integrins control the formation of cell chains in the adult rostral migratory stream. J. Neurosci. *27*, 2704–2717.

Britanova, O., de Juan Romero, C., Cheung, A., Kwan, K.Y., Schwark, M., Gyorgy, A., Vogel, T., Akopov, S., Mitkovski, M., Agoston, D., et al. (2008). Satb2 is a postmitotic determinant for upper-layer neuron specification in the neocortex. Neuron *57*, 378–392.

Cubelos, B., Sebastián-Serrano, A., Kim, S., Moreno-Ortiz, C., Redondo, J.M., Walsh, C.A., and Nieto, M. (2008). Cux-2 controls the proliferation of neuronal intermediate precursors of the cortical subventricular zone. Cereb. Cortex *18*, 1758–1770.

Eckler, M.J., Nguyen, T.D., McKenna, W.L., Fastow, B.L., Guo, C., Rubenstein, J.L.R., and Chen, B. (2015). Cux2-positive radial glial cells generate diverse subtypes of neocortical projection neurons and macroglia. Neuron *86*, this issue, 1100–1108.

Fame, R.M., MacDonald, J.L., and Macklis, J.D. (2011). Development, specification, and diversity of callosal projection neurons. Trends Neurosci. *34*, 41–50.

Franco, S.J., Martinez-Garay, I., Gil-Sanz, C., Harkins-Perry, S.R., and Müller, U. (2011). Reelin regulates cadherin function via Dab1/Rap1 to control neuronal migration and lamination in the neocortex. Neuron *69*, 482–497.

Franco, S.J., Gil-Sanz, C., Martinez-Garay, I., Espinosa, A., Harkins-Perry, S.R., Ramos, C., and Müller, U. (2012). Fate-restricted neural progenitors in the mammalian cerebral cortex. Science *337*, 746–749.

Gao, P., Postiglione, M.P., Krieger, T.G., Hernandez, L., Wang, C., Han, Z., Streicher, C., Papusheva, E., Insolera, R., Chugh, K., et al. (2014). Deterministic progenitor behavior and unitary production of neurons in the neocortex. Cell *159*, 775–788.

Ge, W.-P., Miyawaki, A., Gage, F.H., Jan, Y.-N., and Jan, L.Y. (2012). Local generation of glia is a major astrocyte source in postnatal cortex. Nature *484*, 376–380.

Gorski, J.A., Talley, T., Qiu, M., Puelles, L., Rubenstein, J.L.R., and Jones, K.R. (2002). Cortical excitatory neurons and glia, but not GABAergic neurons, are produced in the Emx1-expressing lineage. J. Neurosci. *22*, 6309–6314.

Guenthner, C.J., Miyamichi, K., Yang, H.H., Heller, H.C., and Luo, L. (2013). Permanent genetic access to transiently active neurons via TRAP: targeted recombination in active populations. Neuron *78*, 773–784.

Guo, C., Eckler, M.J., McKenna, W.L., McKinsey, G.L., Rubenstein, J.L.R., and Chen, B. (2013). Fezf2 expression identifies a multipotent progenitor for neocortical projection neurons, astrocytes, and oligodendrocytes. Neuron *80*, 1167–1174.

Hayashi, S., and McMahon, A.P. (2002). Efficient recombination in diverse tissues by a tamoxifen-inducible form of Cre: a tool for temporally regulated gene activation/inactivation in the mouse. Dev. Biol. *244*, 305–318.

Koop, K.E., MacDonald, L.M., and Lobe, C.G. (1996). Transcripts of Grg4, a murine groucho-related gene, are detected in adjacent tissues to other murine neurogenic gene homologues during embryonic development. Mech. Dev. *59*, 73–87.

Madisen, L., Zwingman, T.A., Sunkin, S.M., Oh, S.W., Zariwala, H.A., Gu, H., Ng, L.L., Palmiter, R.D., Hawrylycz, M.J., Jones, A.R., et al. (2010). A robust and high-throughput Cre reporting and characterization system for the whole mouse brain. Nat. Neurosci. *13*, 133–140.

Miyata, T., Kawaguchi, A., Saito, K., Kawano, M., Muto, T., and Ogawa, M. (2004). Asymmetric production of surface-dividing and non-surface-dividing cortical progenitor cells. Development *131*, 3133–3145.

Molyneaux, B.J., Arlotta, P., Fame, R.M., MacDonald, J.L., MacQuarrie, K.L., and Macklis, J.D. (2009). Novel subtype-specific genes identify distinct subpopulations of callosal projection neurons. J. Neurosci. *29*, 12343–12354.

Nieto, M., Monuki, E.S., Tang, H., Imitola, J., Haubst, N., Khoury, S.J., Cunningham, J., Götz, M., and Walsh, C.A. (2004). Expression of Cux-1 and Cux-2 in the subventricular zone and upper layers II-IV of the cerebral cortex. J. Comp. Neurol. *479*, 168–180.

Noctor, S.C., Martínez-Cerdeño, V., Ivic, L., and Kriegstein, A.R. (2004). Cortical neurons arise in symmetric and asymmetric division zones and migrate through specific phases. Nat. Neurosci. *7*, 136–144.

Sohur, U.S., Padmanabhan, H.K., Kotchetkov, I.S., Menezes, J.R.L., and Macklis, J.D. (2014). Anatomic and molecular development of corticostriatal projection neurons in mice. Cereb. Cortex *24*, 293–303.

Vasistha, N.A., García-Moreno, F., Arora, S., Cheung, A.F.P., Arnold, S.J., Robertson, E.J., and Molnár, Z. (2014). Cortical and clonal contribution of Tbr2 expressing progenitors in the developing mouse brain. Cereb. Cortex. Published online June 13, 2014. http://dx.doi.org/10.1093/cercor/bhu125.

Wu, S.-X., Goebbels, S., Nakamura, K., Nakamura, K., Kometani, K., Minato, N., Kaneko, T., Nave, K.-A., and Tamamaki, N. (2005). Pyramidal neurons of upper cortical layers generated by NEX-positive progenitor cells in the subventricular zone. Proc. Natl. Acad. Sci. USA *102*, 17172–17177.

Yang, G., Smibert, C.A., Kaplan, D.R., and Miller, F.D. (2014). An eIF4E1/4E-T complex determines the genesis of neurons from precursors by translationally repressing a proneurogenic transcription program. Neuron *84*, 723–739.

Zervas, M., Millet, S., Ahn, S., and Joyner, A.L. (2004). Cell behaviors and genetic lineages of the mesencephalon and rhombomere 1. Neuron *43*, 345–357.

Zimmer, C., Tiveron, M.-C., Bodmer, R., and Cremer, H. (2004). Dynamics of Cux2 expression suggests that an early pool of SVZ precursors is fated to become upper cortical layer neurons. Cereb. Cortex *14*, 1408–1420.

Neuron

Supplemental Information

Lineage Tracing Using *Cux2-Cre* and *Cux2-CreERT2* Mice

Cristina Gil-Sanz, Ana Espinosa, Santiago P. Fregoso, Krista K. Bluske, Christopher L. Cunningham, Isabel Martinez-Garay, Hongkui Zeng, Santos J. Franco, and Ulrich Müller

INVENTORY OF SUPPLEMENTAL INFORMATION

1. Supplemental Experimental Procedures

2. Supplemental References

3. Supplemental Figures S1-S3

SUPPLEMENTAL EXPERIMENTAL PROCEDURES

Mice

Cux2-Cre (Franco et al., 2012; 2011), *Cux2-CreERT2* (Franco et al., 2012), *Neurod6-Cre* (Goebbels et al., 2006), *Emx1-Cre* (*B6.129S2-Emx1tm1(cre)Krj*) (Gorski et al., 2002), *Rosa26-LacZ (Gt(ROSA)26Sor)* (Friedrich and Soriano, 1991), *Z/EG (Tg(ACTB-Bgeo/GFP)21Lbe)* (Novak et al., 2000), *Ai9* (Madisen et al., 2010) and *Rosa26-NZG* (*Gt(ROSA)26Sortm1(CAG-lacZ,-EGFP)Glh/J*) (Yamamoto et al., 2009) mice have been previously described. Induction of Cre-activity in *Cux2-CreERT2* mice was achieved by intraperitoneal injection of pregnant dams with 4-OHT (Sigma) (1 mg/20 g of body weight, dissolved as described (Guenthner et al., 2013), or with tamoxifen exactly as described (Franco et al., 2012). For postnatal analysis of induced animals, pups were delivered by cesarean section at E19.5 and provided with a foster mother until analysis.

Mouse genetic background and breeding

The *Cre* and *CreERT2* transgenes were knocked into the endogenous start site in exon 4 of the *Cux2* gene by homologous recombination in *C57BL/6*-derived ES cells. Positive clones were injected into *C57BL/6J-Tyr c-2J* blastocysts and the resulting chimeras were then mated to *C57BL/6J-Tyr c-2J* females to obtain germline transmission. Heterozygous F1 mice were mated with *B6.Cg-Tg(ACTFLPe)* mice (Rodríguez et al., 2000) to remove the *PGK-Neo* selection cassette and the resulting F2 offspring were subsequently mated to *C57BL/6J* mice to remove the *FLPe* transgene.

All animals used for analyses in Figs. 2-3 and S2-S3 were heterozygous for the Cre allele (*Cux2*$^{+/Cre}$, *Cux2*$^{+/CreERT2}$ or *Neurod6*$^{+/Cre}$) and heterozygous/hemizygous for the Reporter allele (*Ai9*$^{+/fl}$, *Rosa26-LacZ*$^{+/fl}$ or *Z/EG*$^{+/-}$). For Fig. 1A-B and E, "Original" and "Sparse" data were generated by crossing *Cux2*$^{Cre/Cre}$ x *Ai9*$^{fl/fl}$ animals, both on congenic *C57BL/6J* backgrounds. The "Recovered" data in Fig. 1B were generated by first outcrossing *Cux2*$^{Cre/Cre}$ mice to ICR mice for 3 generations, then crossing these *Cux2*$^{+/Cre}$ mice to *Ai9*$^{fl/fl}$ animals on the congenic *C57BL/6J* background. For Fig. 1C-D and F, "Original" and "Expanded" data were generated by crossing *B6.Cg-Cux2*$^{Cre/Cre}$ x *Rosa26*$^{NZG/NZG}$ animals that were on a congenic *FVB/NJ* background. The "Recovered" data in Fig. 1D and F were generated by first outcrossing *Cux2*$^{Cre/Cre}$ mice to *FVB/NJ* mice for 5 generations, then crossing these *Cux2*$^{+/Cre}$ mice to *Rosa26*$^{NZG/NZG}$ animals on the congenic *FVB/NJ* background.

Data in Fig. S1A, C are from *Cux2*$^{+/Cre}$*;Ai14*$^{+/fl}$ animals generated by crossing *Cux2*$^{+/Cre}$ mice to *Ai14*$^{fl/fl}$ animals, both on congenic *C57BL/6J*. Data in Fig. S1D are from *Cux2*$^{+/Cre}$*;Ai14*$^{+/fl}$ animals generated by crossing *Cux2*$^{+/Cre}$*;Ai14*$^{+/fl}$ animals to wild-type *C57BL/6J* mice. Data in Fig. S1E-F are from offspring resulting from crossing *B6.Cg-Cux2*$^{+/Cre}$*;Ai9*$^{+/fl}$ (generated as described above) to wild-type *C57BL/6J* mice Data in the left panels of Fig. S1G are from *Cux2*$^{+/Cre}$;*Rosa26*$^{+/NZG}$ generated by crossing *Cux2*$^{Cre/Cre}$ mice to *FVB/NJ* mice for 3 generations, then crossing these *Cux2*$^{+/Cre}$ mice to *Rosa26*$^{+/NZG}$ animals. Data in the center and right panels of Fig. S1G are from *Cux2*$^{+/Cre}$;*Rosa26*$^{+/ZG}$ and *Cux2*$^{+/+}$;*Rosa26*$^{+/ZG}$ mice, respectively, which were generated by crossing *Cux2*$^{+/Cre}$;*Rosa26*$^{+/NZG}$ mice (generated as described above) to wild-type *FVB/NJ* mice.

Immunohistochemistry and *in utero* electroporation

Embryonic brains were fixed in 4 % paraformaldehyde (PFA) overnight at 4°C. Postnatal

mice were transcardially perfused with 4% PFA and brains postfixed in 4% PFA for 2 hours at 4°C. Brains were sectioned coronally at 50, 75 or 100 μm with a vibrating microtome (VT1200S; Leica). Immunostaining was performed as described and using the same antibodies (Franco et al., 2012; Gil-Sanz et al., 2013), with the addition of anti-Aldh1L1 (Antibodies Inc.), anti-Cre (Covance), anti-Parvalbunin (Swant), anti-RFP (LifeSpan Biosciences), anti-Somatostatin (Abcam), anti-Tle4 rabbit polyclonal (Abcam). In utero electroporations using the Cre responsive plasmid CβA-Flex (Franco et al., 2012) were carried out as described (Franco et al., 2012; Gil-Sanz et al., 2013). Confocal images were captured using a Nikon C2 or a Nikon-A1 laser-scanning confocal microscope system and widefield images were captured on a Nikon Eclipse 80i microscope.

Quantification of recombination and molecular markers

For the Sabt2 and Ctip2 double immunostainings in the *Cux2-Cre;Ai9* mice, at least 3 histological sections from 3 different animals at 3 distinct rostro-caudal levels were analyzed in the medio-lateral part of the neocortex comprising primarily the somatosensory cortex. Confocal optical sections were used for quantification. Cells were first categorized by molecular marker expression (single-positive for either marker or double-positive) and then classified as recombined or not based on tdTomato expression. 2902 cells were analyzed in contiguous columns spanning the region between layer I and the white matter. Values are mean ± SEM. For analysis of interneurons in the *Cux2-Cre;Rosa26-LacZ* mice, 3 sagittal sections from 2 different animals at distinct rostro-caudal levels of the neocortex were analyzed. The proportion of recombined interneurons, the proportion Ctip2$^+$ cells that were interneurons and the proportion of the recombined Ctip2$^+$ cells that were interneurons were calculated. More

than 1200 cells were quantified in contiguous columns spanning the region between layer I and the white matter. Values are mean ± SEM. For Satb2 and Ctip2 double immunostaings in the *Cux2-CreERT2;Ai9* mice 4-6 serial sections from each of 9 mice injected with 4-OHT were analyzed. Confocal optical sections were used for quantification. The total number of recombined tdTomato$^+$ cells present in the cortical plate were analyzed and classified according to the expression of one marker, both markers or neither marker. A total of 1745 cells were analyzed. Quantifications are presented as percentage of the total number of recombined cells expressing the different combinations of markers. For analysis of interneurons in *Cux2-CreERT2;Ai9* mice, 6-9 serial sections from 2 mice injected with 4-OHT were analyzed. Confocal optical sections were used for quantification. The total number of recombined tdTomato$^+$ cells present in the cortical plate were analyzed and classified according to the expression of one marker or both markers. A total of 265 cells were analyzed. Values are mean ± SEM. For quantifications of layer distribution in sparsely recombined *Cux2-Cre;Ai9* brains, 502 cells were quantified from 3 animals. For *Cux2-Cre;Rosa-NZG* mice, 3 sections from each of at least 2 animals were used to quantify >2100 cells for each condition. Layer positions of recombined cells were quantified separately for somatosensory cortex and motor cortex, but did not show significant differences between areas and were therefore combined in the final counts. Values are mean ± SEM.

SUPPLEMENTAL REFERENCES

Franco, S.J., Gil-Sanz, C., Martinez-Garay, I., Espinosa, A., Harkins-Perry, S.R., Ramos, C., and Müller, U. (2012). Fate-restricted neural progenitors in the mammalian cerebral cortex. Science *337*, 746–749.

Franco, S.J., Martinez-Garay, I., Gil-Sanz, C., Harkins-Perry, S.R., and Müller, U. (2011). Reelin regulates cadherin function via Dab1/Rap1 to control neuronal migration and lamination in the neocortex. Neuron *69*, 482–497.

Friedrich, G., and Soriano, P. (1991). Promoter traps in embryonic stem cells: a genetic screen to identify and mutate developmental genes in mice. Genes Dev *5*, 1513–1523.

Gil-Sanz, C., Franco, S.J., Martinez-Garay, I., Espinosa, A., Harkins-Perry, S., and Müller, U. (2013). Cajal-Retzius cells instruct neuronal migration by coincidence signaling between secreted and contact-dependent guidance cues. Neuron *79*, 461–477.

Goebbels, S., Bormuth, I., Bode, U., Hermanson, O., Schwab, M.H., and Nave, K.-A. (2006). Genetic targeting of principal neurons in neocortex and hippocampus of NEX-Cre mice. Genesis *44*, 611–621.

Gorski, J.A., Talley, T., Qiu, M., Puelles, L., Rubenstein, J.L.R., and Jones, K.R. (2002). Cortical excitatory neurons and glia, but not GABAergic neurons, are produced in the Emx1-expressing lineage. J Neurosci *22*, 6309–6314.

Guenthner, C.J., Miyamichi, K., Yang, H.H., Heller, H.C., and Luo, L. (2013). Permanent genetic access to transiently active neurons via TRAP: targeted recombination in active populations. Neuron *78*, 773–784.

Madisen, L., Zwingman, T.A., Sunkin, S.M., Oh, S.W., Zariwala, H.A., Gu, H., Ng, L.L., Palmiter, R.D., Hawrylycz, M.J., Jones, A.R., et al. (2010). A robust and high-throughput Cre reporting and characterization system for the whole mouse brain. Nat Neurosci *13*, 133–140.

Novak, A., Guo, C., Yang, W., Nagy, A., and Lobe, C.G. (2000). Z/EG, a double reporter mouse line that expresses enhanced green fluorescent protein upon Cre-mediated excision. Genesis *28*, 147–155.

Rodríguez, C.I., Buchholz, F., Galloway, J., Sequerra, R., Kasper, J., Ayala, R., Stewart, A.F., and Dymecki, S.M. (2000). High-efficiency deleter mice show that FLPe is an alternative to Cre-loxP. Nat Genet *25*, 139–140.

Yamamoto, M., Shook, N.A., Kanisicak, O., Yamamoto, S., Wosczyna, M.N., Camp, J.R., and Goldhamer, D.J. (2009). A multifunctional reporter mouse line for Cre- and FLP-dependent lineage analysis. Genesis *47*, 107–114.

Figure S1, related to Figure 1 (Gil-Sanz, et al.)

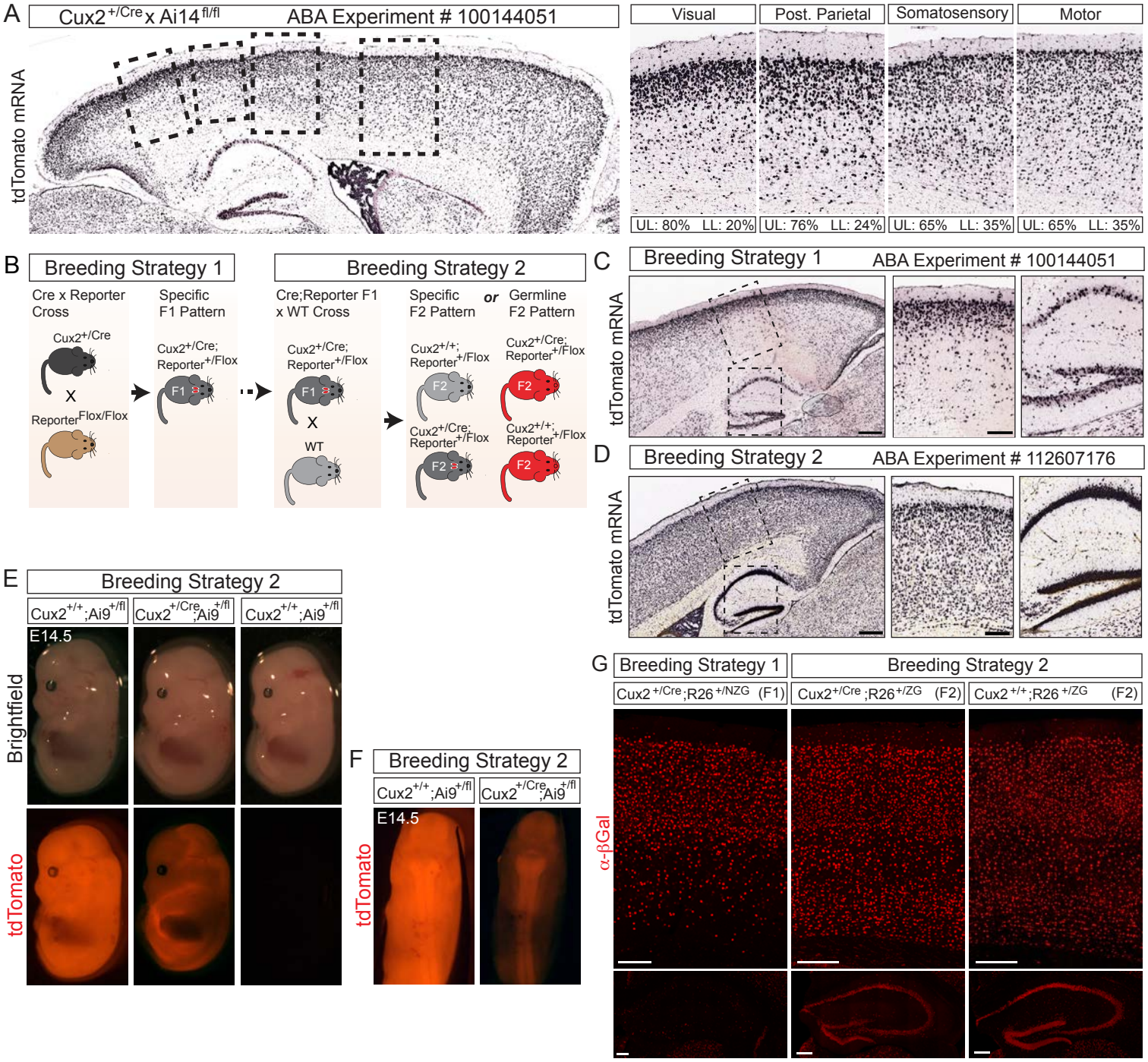

Figure S1. **Related to Figure 1**. ***Cux2*** **genetic locus is active in the developing germline.** (**A**) Sagittal sections displaying *tdTomato* in situ hybridizations in the brains of a *Cux2-Cre;Ai14* mouse generated by Cre x Reporter breeding as in Breeding Strategy 1 shown in (B). Images at right are higher magnifications of insets in overview at left. Quantification is percentage of total recombined cells that are found in upper layers 2-4 (UL) or in lower layers 5-6 (LL). (**B**) Different breeding strategies used to generate mice for analysis. Breeding Strategy 1 involves breeding a *Cux2-Cre* heterozygous animal to a homozygous Reporter animal (i.e., $Ai14^{fl/fl}$, $Ai9^{fl/fl}$ or $Rosa26\text{-}NZG^{fl/fl}$) to produce double heterozygous F1 animals that exhibit the layer-specific recombination pattern. For Breeding Strategy 2, these double heterozygous animals were then crossed to WT mice to produce F2 animals. Some F2 mice showed the expected specific recombination patterns, whereas others exhibited ubiquitous reporter expression indicating germline transmission of the recombined reporter allele. (**C**) Sagittal sections displaying *tdTomato* in situ hybridizations in the brains of a *Cux2-Cre;Ai14* mouse generated by Breeding Strategy 1 as described in (B). Note the restricted recombination patterns in the neocortex (left, middle panels) and the hippocampus (right panel). (**D**) Sagittal sections displaying *tdTomato* in situ hybridizations in the brains of a *Cux2-Cre;Ai14* mouse generated by Breeding Strategy 2 as described in (B). Note the equal distribution of $tdTomato^{+}$ cells throughout all layers of the neocortex and the extensive recombination throughout the hippocampus. (**E**) Wide-field images (transmitted light and fluorescence) showing the F2 offspring resulting from Breeding Strategy 2 shown in (B). Note that some embryos without Cre have no recombination (right panels) and some with Cre exhibit the normal recombination pattern (center panels), whereas others display widespread recombination even without the Cre allele (left panels), indicating germline recombination. (**F**) Fluorescence images of one germline recombined embryo (left) showing widespread recombination and a normal recombined embryo (right) displaying

fluorescence in the brain and spinal cord. (**G**) Confocal images displaying the neocortex (top) and the hippocampus (bottom) of animals with normal recombination (Breeding Strategy 1) and animals showing germline recombination (Breeding Strategy 2). Note that essentially all cells present in these animals appear to be recombined, even in the absence of Cre. Scale bars: (C-D) 400 μm; (G) 200 μm.

Figure S2, related to Figure 2 (Gil-Sanz et al.)

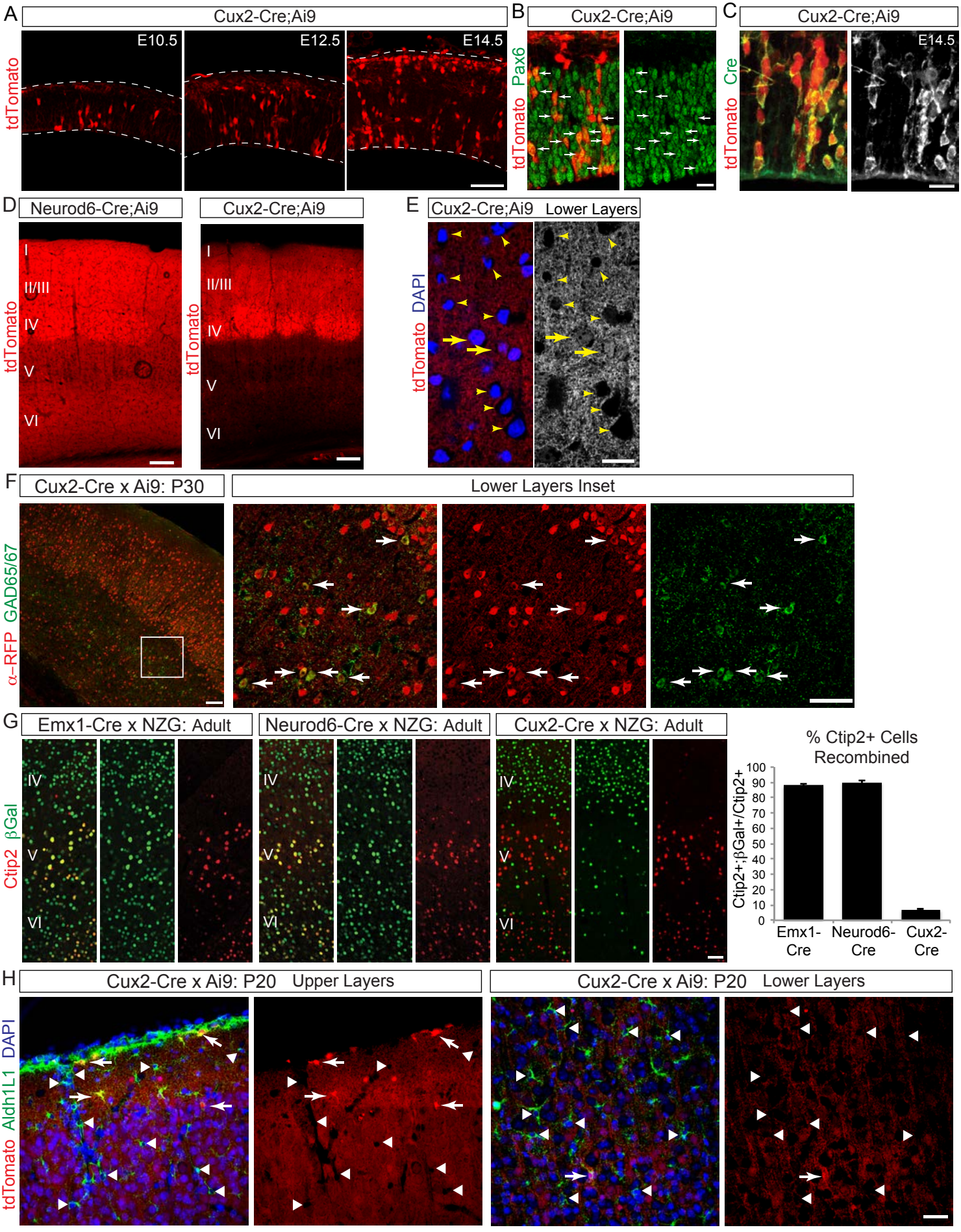

Figure S2. Related to Figure 2. *Cux2-Cre* is expressed by a subpopulation of interneurons and astrocytes. (**A**) Recombination patterns in the neocortex at E10.5, E12.5 and E14.5 in *Cux2-Cre*;*Ai9* mice. Note the presence of recombined cells with RGC morphology. (**B**) Confocal images of the VZ of a *Cux2-Cre;Ai9* embryo at E12.5. Arrows highlight recombined tdTomato$^+$ cells (red) that express Pax6 (green). (**C**) Sections of *Cux2-Cre;Ai9* VZ at E14.5 stained with α-Cre (green) to reveal expression in recombined tdTomato$^+$ cells (red). (**D**) Recombination patterns in the neocortex at P30 from *Neurod6-Cre* and *Cux2-Cre* crossed to Ai9 reporters. (**E**) Coronal section of a *Cux2-Cre*;*Ai9* brain showing that the majority of fluorescence signal in lower layers is in the neuropil from upper layer neurons. Nuclei are stained with DAPI (blue). (**F**) Coronal sections from a *Cux2-Cre;Ai9* neocortex immunostained with the interneuron marker Gad65/67 (green) and an antibody against RFP (red) to enhance the soma staining in the recombined cells. Boxed inset is shown enlarged at right to demonstrate recombined interneurons (arrows). (**G**) Coronal neocortical sections from different Cre mice crossed to the *Rosa26-NZG* reporter, immunostained for Ctip2 (red) and βGal (green). Note that the majority of Ctip2$^+$ cells are recombined (βGal$^+$) in *Emx1-Cre;NZG* and *Neurod6-Cre;NZG* mice, whereas very few Ctip2$^+$ cells are recombined in *Cux2-Cre;NZG* brains. Graph shows the percentage of Ctip2$^+$ cells that are recombined in each strain, ± SEM. (**H**) Coronal section from a *Cux2-Cre;Ai9* neocortex immunostained with the general astrocyte marker Aldlh1L1 (green). tdTomato$^+$ recombined cells are shown in red and DAPI-stained nuclei in blue. Note that some astrocytes are recombined (arrows), but the vast majority of astrocytes are not recombined, as revealed by the absence of tdTomato signal (arrowheads). Abbrev. I-VI: layers I-VI. Scale bars: (A, D) 100 μm; (B, C) 25 μm; (E) 20 μm; (F) 100 μm, insets 50 μm; (G, H) 50 μm.

Figure S3, related to Figure 3 (Gil-Sanz et al.)

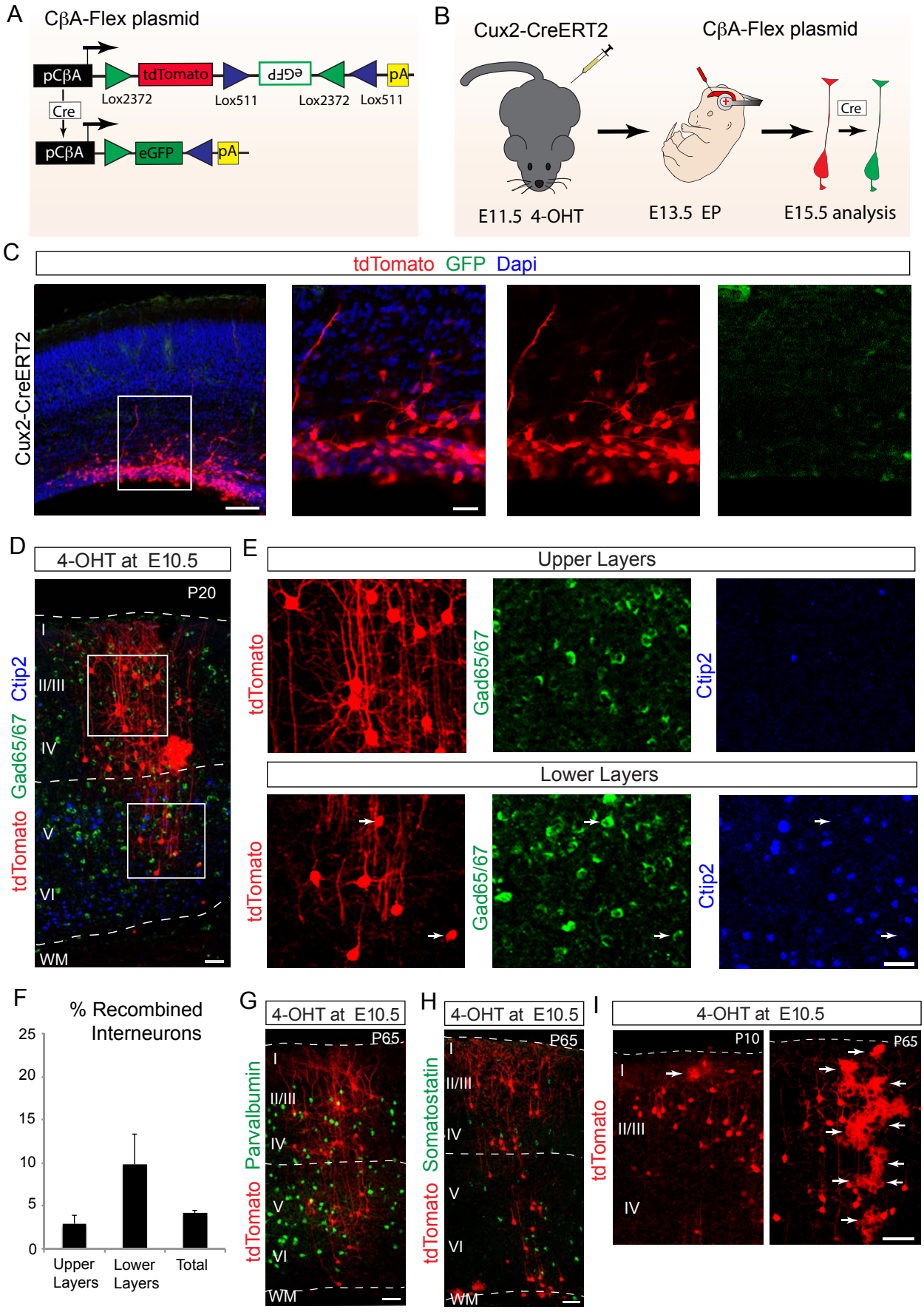

Figure S3. Related to Figure 3. *Cux2-CreERT2*$^{+}$ progenitors generate a small subpopulation of cortical interneurons and astrocytes. (**A**) Schematic of the CβA-Flex plasmid. This plasmid drives differential expression of tdTomato or EGFP upon Cre recombination. (**B**) Schematic of the strategy used to evaluate the duration of the activity of tamoxifen to mediate Cre recombination. *Cux2-CreERT2* pregnant dams were injected with 4-OHT at E11.5 and 2 days later the embryos were electroporated with the Cre responsive plasmid. Brains were analyzed 2 days after electroporation. (**C**) Confocal images of embryonic brains showing the neocortex after performing the experiment described in (B). Non-recombined cells express tdTomato (red) and recombined cells express GFP (green). DAPI-stained nuclei are in blue. Note the absence of EGFP expression in the ventricular zone of the electroporated brains. (**D**) Overview of the adult neocortex from a *Cux2-CreERT2;Ai9* mouse injected with 4-OHT at E10.5, immunostained with the interneuron marker Gad65/67 (green) and Ctip2 (blue). tdTomato^{+} recombined cells are in red. (**E**) Higher magnification of the boxed areas in (D). (**F**) Quantification (mean ± SEM) of the percentage of recombined interneurons present in the *Cux2-CreERT2;Ai9* neocortex after 4-OHT injections at E10.5. (**G**-**H**) Confocal images of the *Cux2-CreERT2;Ai9* neocortex after 4-OHT injection at E10.5, immunostained with interneuron markers parvalbumin (G) and somatostatin (H) (green), tdTomato recombined cells are red. (**I**) Confocal images of the *Cux2-CreERT2;Ai9* neocortex after injection with 4-OHT at E10.5, analyzed at P10 or P65. Note the presence of a small number of astrocytes (arrow) at P10 and larger numbers of astrocytes present in groups at P65 (arrows). Scale bars: (D, G-H) 100 μm; (E) 50 μm.